

- GILMORE, C. J. (1984). *J. Appl. Cryst.* **17**, 42–46.
- GILMORE, C. J. & BROWN, S. R. (1988). *Acta Cryst.* **A44**, 1018–1021.
- GRIGG, R., KEMP, J., SHELDRIK, G. M. & TROTTER, J. (1978). *Chem. Commun.* pp. 109–111.
- HAUPTMAN, H. (1974). *Acta Cryst.* **A30**, 822–829.
- HOPF, H., LEHNE, V. & JONES, P. G. (1990). In preparation.
- HULL, S. E. & IRWIN, M. J. (1978). *Acta Cryst.* **A34**, 863–870.
- JONES, P. G., SHELDRIK, G. M., GLÜSENKAMP, K. H. & TIETZE, L. F. (1980). *Acta Cryst.* **B36**, 481–483.
- KARLE, J. & KARLE, I. L. (1966). *Acta Cryst.* **21**, 849–859.
- KIRKPATRICK, S., GELATT, C. D. & VECCHI, M. P. (1983). *Science*, **220**, 671–680.
- KURIYAN, J., BRÜNGER, A. T., KARPLUS, M. & HENDRICKSON, W. A. (1989). *Acta Cryst.* **A45**, 396–409.
- METROPOLIS, N., ROSENBLUTH, A. W., ROSENBLUTH, M. N., TELLER, A. H. & TELLER, E. (1953). *J. Chem. Phys.* **21**, 1087–1092.
- OLIVER, J. D. & STRICKLAND, L. C. (1984). *Acta Cryst.* **C40**, 820–824.
- POYSER, J. P., EDWARDS, P. L., ANDERSON, J. R., HURSTHOUSE, M. B., WALKER, N. P. C., SHELDRIK, G. M. & WHALLEY, A. J. S. (1986). *J. Antibiotics*, **39**, 167–169.
- ROBERTS, P. J., PETTERSEN, R. C., SHELDRIK, G. M., ISAACS, N. W. & KENNARD, O. (1973). *J. Chem. Soc. Perkin Trans. 2*, pp. 1978–1984.
- ROBINSON, W. T. & SHELDRIK, G. M. (1988). *Crystallographic Computing 4: Techniques and New Technologies*, edited by N. W. ISAACS & M. R. TAYLOR, pp. 366–377. International Union of Crystallography, Oxford Univ. Press.
- SCHENK, H. (1972). *Acta Cryst.* **A28**, 412–421.
- SCHENK, H. (1974). *Acta Cryst.* **A30**, 477–481.
- SHELDRIK, G. M. (1982). *Computational Crystallography*, edited by D. SAYRE, pp. 506–514. Oxford: Clarendon Press.
- SHELDRIK, G. M. (1985). *Crystallographic Computing 3: Data Collection, Structure Determination, Proteins, and Databases*, edited by G. M. SHELDRIK, C. KRÜGER & R. GODDARD, pp. 184–189. Oxford: Clarendon Press.
- WOOLFSON, M. M. (1987). *Acta Cryst.* **A43**, 593–612.
- YAO JIA-XING (1981). *Acta Cryst.* **A37**, 642–644.

*Acta Cryst.* (1990). **A46**, 473–478

## On the Determination of Quasicrystal Structures

BY XIANG SHI-BIN, LI FANG-HUA AND FAN HAI-FU

*Institute of Physics, Chinese Academy of Sciences, Beijing, China*

(Received 21 August 1989; accepted 24 January 1990)

### Abstract

A possible approach to direct phasing of quasicrystal diffraction data is described. The data are first converted to a set of structure-factor amplitudes of a multidimensional crystal. The Patterson function of the quasicrystal is used to derive the converting factor. A direct method is then used to solve the phase problem in multi-dimensional space. The method has been tested with a hypothetical one-dimensional quasicrystal yielding a satisfactory result.

### Introduction

The recently discovered quasicrystals (Shechtman, Blech, Gratias & Cahn, 1984) belong to a new kind of substance between the crystalline and amorphous states. They have long-range orientational order as well as long-range quasiperiodicity. The inconsistency of their symmetry with classical crystallography has drawn great attention from condensed-matter physicists and chemists. Determination of quasicrystal structures is important for understanding the properties or for exploring the applications of quasicrystals. So far quasicrystal structure determination has mainly been performed by trial-and-error methods. One must first propose a structure model,

calculate the diffraction intensities and then compare with the experimental data. This is a tedious process; it resembles the structure analysis of crystals in the early days. During the last two decades X-ray analysis of crystal structures has achieved great progress owing to the development of direct methods (Woolfson, 1987). Hence it is worth trying to apply direct methods to quasicrystal structures. However, the task is far from straightforward, since quasicrystals do not possess periodicity in the sense of classical crystallography. Use of direct methods in quasicrystal structure analysis was proposed by Li Fang-hua, Wang Li-chen & Fan Hai-fu (1987). A structure-factor relation for quasicrystals has been derived and a preliminary test result has been obtained. In the previous study, the shape factor for constructing a quasicrystal from a multi-dimensional (MD) crystal is assumed to be known in advance. However this is not true in practice. In order that direct methods can be useful in practice, this problem remains to be solved. In this paper, a method which makes use of the Patterson function is proposed to determine the shape factor. This enables the conversion of diffraction data from a three-dimensional (3D) quasicrystal to the corresponding MD crystal. Direct methods can then be used to solve the phase problem in MD space.

### Principle

Quasicrystals yield sharp diffraction peaks which do not have simple indices in 3D reciprocal space. In principle, direct methods can still be used if a huge unit cell is chosen. However, the large number of atoms in such a unit cell makes the problem too complicated. Hence it would be better to have an alternative representation for quasicrystal structures. According to Bak (1986) and Janssen (1986) the diffraction pattern of a 3D quasicrystal can be regarded as the projection of a MD-weighted reciprocal lattice. Each reciprocal-lattice point has a weight equal to the corresponding intensity diffracted from the quasicrystal. The position vector of a lattice point can be expressed as

$$\hat{\mathbf{H}} = \sum_{i=1}^n h_i \mathbf{b}_i, \quad (1)$$

where the  $\mathbf{b}_i$ 's are translation vectors defining the MD reciprocal unit cell, and the  $h_i$ 's are the  $n$  indices of a particular diffraction spot of the quasicrystal; they are all simple integers. On the other hand by a coordinate transform according to the symmetry of the quasicrystal,  $\hat{\mathbf{H}}$  can also be split into two components  $\mathbf{H}$  and  $\mathbf{H}_\perp$ . The former is the projection of  $\hat{\mathbf{H}}$  onto 3D reciprocal space while the latter is that onto  $(n-3)$ D pseudo-reciprocal space. Both  $\mathbf{H}$  and  $\mathbf{H}_\perp$  do not have simple indices. Now a 3D quasicrystal can be described as a 3D section of a MD crystal. The corresponding structure factors are denoted by  $F_q(\hat{\mathbf{H}})$ , the magnitude of which can be derived from the diffraction intensity of the quasicrystal. The unit cell is defined by a set of translation vectors  $\mathbf{a}_i$ , which is the reciprocal of  $\mathbf{b}_i$ . A position vector in the MD crystal can be expressed as

$$\hat{\mathbf{r}} = \sum_{i=1}^n x_i \mathbf{a}_i. \quad (2)$$

$\hat{\mathbf{r}}$  can also be split into two components  $\mathbf{r}$  and  $\mathbf{r}_\perp$ . The former is the projection of  $\hat{\mathbf{r}}$  onto 3D physical space while the latter is that onto  $(n-3)$ D pseudo-space. The MD crystal shows no periodicity in either physical space or pseudo-space alone. It should be noticed that the MD crystal described above corresponds to a special MD lattice, the nodes of which are not geometrical points. They have a particular shape in pseudo-space defined by a window function  $w(\mathbf{r}_\perp)$  which equals unity or zero depending on whether  $\mathbf{r}_\perp$  lies inside or outside a certain region around the lattice points. Atoms in such a MD crystal are then spread in the pseudo-space as they convolute with the window function. In order that direct methods can be applied, it is necessary to convert the above MD crystal to one having a normal lattice with geometrical points as nodes. The structure factor of this MD crystal is denoted by  $F(\hat{\mathbf{H}})$ . The relation

between  $F_q(\hat{\mathbf{H}})$  and  $F(\hat{\mathbf{H}})$  can be written as

$$F_q(\hat{\mathbf{H}}) = S(\mathbf{H}_\perp)F(\hat{\mathbf{H}}), \quad (3)$$

where  $S(\mathbf{H}_\perp)$  is a shape factor which is the Fourier transform of the window function  $w(\mathbf{r}_\perp)$ . Direct methods have proved successful for solving incommensurate modulated structures in MD space (Hao Quan, Liu Yi-wei & Fan Hai-fu, 1987). They can also be used to solve the phase problem of quasicrystals provided we can derive the shape factor  $S(\mathbf{H}_\perp)$  from experiment. This can be done as follows. Square both sides of (3). Then by the convolution theorem we have

$$P_q(\mathbf{r}, \mathbf{r}_\perp) = P(\mathbf{r}, \mathbf{r}_\perp) * [w(\mathbf{r}_\perp) * w(\mathbf{r}_\perp)] \quad (4)$$

where  $P_q(\mathbf{r}, \mathbf{r}_\perp)$  is the inverse Fourier transform of  $|F_q(\mathbf{H}, \mathbf{H}_\perp)|^2$ , *i.e.* the Patterson function of the MD crystal corresponding to a special lattice, nodes of which have the shape defined by  $w(\mathbf{r}_\perp)$ .  $P(\mathbf{r}, \mathbf{r}_\perp)$  is the inverse Fourier transform of  $|F(\mathbf{H}, \mathbf{H}_\perp)|^2$ , *i.e.* the Patterson function of the MD crystal corresponding to a normal lattice with geometrical points as nodes. '\*' denotes the convolution operation.  $w(\mathbf{r}_\perp)$  is the inverse Fourier transform of  $S(\mathbf{H}_\perp)$ . Our task is to find the boundary of  $w(\mathbf{r}_\perp)$ . Consider a region near  $P(0, 0)$ . Then  $P(0, \mathbf{r}_\perp)$  will be a delta function centred on  $\mathbf{r}_\perp = 0$ . Hence within a region near the origin of the MD space, we can write

$$P_q(0, \mathbf{r}_\perp) = Cw(\mathbf{r}_\perp) * w(\mathbf{r}_\perp), \quad (5)$$

where  $C$  is a constant.  $w(\mathbf{r}_\perp) * w(\mathbf{r}_\perp)$  has a maximum at  $\mathbf{r}_\perp = 0$ . It gradually falls to zero, or in practice falls to a base level, as  $|\mathbf{r}_\perp|$  increases to a value equal to the width of  $w(\mathbf{r}_\perp)$  along the direction of  $\mathbf{r}_\perp$ . Hence we can determine the boundary of  $w(\mathbf{r}_\perp)$  from the shape of the Patterson-origin peak. In summary a quasicrystal structure can be determined through the following steps:

(1) Index the diffraction pattern in MD space, *i.e.* find the corresponding MD reciprocal lattice and the relation between physical space and MD space.

(2) Determine the shape factor  $S(\mathbf{H}_\perp)$  from  $P_q(0, \mathbf{r}_\perp)$ .

(3) Convert  $|F_q(\hat{\mathbf{H}})|$  to the normalized structure factors  $|E(\hat{\mathbf{H}})|$  of the corresponding MD crystal.

(4) Solve the MD crystal by direct methods.

(5) Cut the MD crystal by physical space to obtain the quasicrystal.

### Test model

In the following test we use a centrosymmetric 1D quasicrystal model which corresponds to a Fibonacci sequence and is constructed by cutting a 2D square structure with a line - the 1D physical space (see Fig. 1). A position vector in the 2D space is expressed as

$$\hat{\mathbf{r}} = x_1 \mathbf{a}_1 + x_2 \mathbf{a}_2.$$

Both  $\mathbf{a}_1$  and  $\mathbf{a}_2$  have a period  $a = 18.00 \text{ \AA}$ .  $\hat{\mathbf{r}}$  can also

be expressed as

$$\hat{\mathbf{r}} = \mathbf{x} + \mathbf{x}_\perp,$$

where  $\mathbf{x}$  is defined in the 1D physical space while  $\mathbf{x}_\perp$  is defined in the 1D pseudo-space perpendicular to  $\mathbf{x}$ . The angle  $\theta$  between  $\mathbf{x}$  and  $\mathbf{x}_1$  is given by

$$\cot \theta = (1 + \sqrt{5})/2.$$

The two segments constructing the Fibonacci sequence are denoted by

$$l_1 = a \cos \theta \quad \text{and} \quad l_2 = a \sin \theta,$$

respectively. Corresponding to the 2D-lattice shown in Fig. 1, there is a 2D reciprocal lattice. The position vector of the lattice points is given by

$$\hat{\mathbf{H}} = h_1 \mathbf{b}_1 + h_2 \mathbf{b}_2,$$

where  $\mathbf{b}_1$  and  $\mathbf{b}_2$  are reciprocal to  $\mathbf{a}_1$  and  $\mathbf{a}_2$ .  $h_1$  and  $h_2$  are the two integer indices for a 2D reciprocal-lattice point.  $\hat{\mathbf{H}}$  can also be expressed as

$$\hat{\mathbf{H}} = \mathbf{H} + \mathbf{H}_\perp,$$

where  $\mathbf{H} = h_1 l_1^* + h_2 l_2^*$  and  $\mathbf{H}_\perp = h_2 l_1^* - h_1 l_2^*$ , in which  $l_1^* = a^* \cos \theta$  and  $l_2^* = a^* \sin \theta$ ; they are the two segments constructing the 1D reciprocal quasilattice.  $a^* = 1/a$  is the period of the 2D reciprocal lattice. The shape factor relating  $F_q(\hat{\mathbf{H}})$  and  $F(\hat{\mathbf{H}})$  then becomes (Li Fang-hua *et al.*, 1987)

$$S(\mathbf{H}_\perp) = \sin \pi \mathbf{H}_\perp (l_1 + l_2) / \pi \mathbf{H}_\perp. \quad (6)$$

The 2D square structure is constructed by convoluting four equal atoms with the 2D square lattice described above. The atomic number is chosen arbitrarily as 25. The absolute coordinates (in ångströms) of the two independent atoms in the coordinate system ( $\mathbf{x}_1, \mathbf{x}_2$ ) are (7.626, 6.155) and (1.910, 2.397), which were chosen by a random generator keeping the condition that in the 1D physical space, no atomic distance should be less than the sum of two atomic radii. In 100 000 random trials, it was found that no structure model with more than two independent atoms can fulfil this condition. This means that for a one-dimensional quasicrystal it is hard to find a model

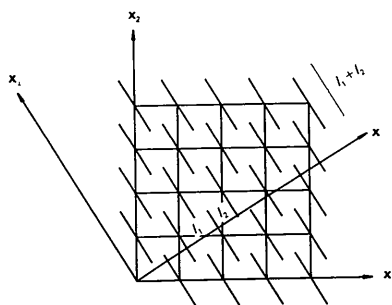


Fig. 1. Construction of 1D quasicrystal by cutting a 2D crystal structure, elucidated by cutting a square lattice to form a Fibonacci sequence.

Table 1. Atomic positions in the 1D quasicrystal

| Atom | $X_m$ | $X_d$ |
|------|-------|-------|
| 1    | 2.88  | 2.88  |
| 2    | 5.58  | 5.57  |
| 3    | 9.72  | 9.73  |
| 4    | 12.42 | 12.42 |
| 5    | 15.05 | 15.04 |
| 6    | 18.19 | 18.20 |
| 7    | 21.89 | 21.88 |
| 8    | 25.03 | 25.04 |
| 9    | 27.65 | 27.66 |
| 10   | 30.36 | 30.35 |
| 11   | 34.49 | 34.50 |
| 12   | 37.20 | 37.19 |
| 13   | 39.82 | 39.81 |
| 14   | 42.97 | 42.97 |
| 15   | 46.66 | 46.66 |
| 16   | 49.80 | 49.82 |
| 17   | 55.13 | 55.12 |
| 18   | 58.28 | 58.28 |
| 19   | 61.97 | 61.97 |
| 20   | 65.12 | 65.13 |
| 21   | 67.74 | 67.75 |
| 22   | 70.45 | 70.43 |
| 23   | 74.58 | 74.59 |
| 24   | 77.28 | 77.28 |
| 25   | 79.91 | 79.90 |
| 26   | 83.05 | 83.06 |
| 27   | 86.75 | 86.74 |
| 28   | 89.89 | 89.90 |
| 29   | 92.52 | 92.52 |
| 30   | 95.22 | 95.21 |

$X_m$ : positions from the model structure (Å).

$X_d$ : positions from the direct-method result (Å).

more complicated than that used in our test with the given unit cell, atomic species,  $\theta$  and  $(l_1 + l_2)$ . By cutting this 2D square structure with the line  $\mathbf{x}$ , we obtained the 1D quasicrystal model. Atomic positions of the first 30 atoms are listed in Table 1. Structure factors,  $F_q(\hat{\mathbf{H}})$ , corresponding to the electron diffraction from the first 10 000 atoms of this 1D quasicrystal at 1 Å resolution were calculated as shown in Table 2. Reflections with intensity less than 1% of the largest have been omitted and were not used throughout the test calculation. Our test was performed by assuming that we know in advance only the following information:

- (1) the 2D structure is centrosymmetric;
  - (2) 2D square unit cell:  $a = 18.00$  Å;
  - (3) the angle  $\theta$  between  $\mathbf{x}$  and  $\mathbf{x}_1$ ;
  - (4) unit-cell contents: four atoms with atomic number equal to 25;
  - (5) the magnitudes of  $F_q(\hat{\mathbf{H}})$  as listed in Table 2.
- All the above information, except (1), is easy to obtain from experiment.

## Test and results

### A. Evaluation of $S(\mathbf{H}_\perp)$

According to (6) the inverse Fourier transform of  $S(\mathbf{H}_\perp)$  is a window function

$$w(\mathbf{x}_\perp) = \begin{cases} 1, & \text{if } |\mathbf{x}_\perp| \leq (l_1 + l_2)/2 \\ 0, & \text{if } |\mathbf{x}_\perp| > (l_1 + l_2)/2. \end{cases}$$

Table 2. Structure factors of the 2D crystal structure converted from the 1D quasicrystal

$$\mathbf{H} = h_1 \mathbf{b}_1 + h_2 \mathbf{b}_2.$$

Signs of structure factors derived from the direct method are exactly the same as those calculated from the model.

| $h_1$ | $h_2$ | $ \mathbf{F}_q(\mathbf{H}) $ | $ \mathbf{F}(\mathbf{H}) $ | $ \mathbf{E}(\mathbf{H}) $ | Sign |
|-------|-------|------------------------------|----------------------------|----------------------------|------|
| 0     | 4     | 31.62                        | 22.26                      | 1.62                       | -    |
| 1     | -1    | 37.67                        | 27.50                      | 0.95                       | +    |
| 1     | 1     | 41.21                        | 2.37                       | 0.14                       | +    |
| 1     | 3     | 44.53                        | 25.40                      | 1.83                       | -    |
| 2     | 0     | 60.95                        | 11.34                      | 0.79                       | +    |
| 2     | 1     | 55.89                        | 2.56                       | 0.18                       | -    |
| 2     | 2     | 71.72                        | 24.86                      | 1.83                       | -    |
| 3     | -1    | 36.72                        | 17.77                      | 1.29                       | +    |
| 3     | 5     | 33.09                        | 18.34                      | 1.95                       | +    |
| 4     | 2     | 156.23                       | 11.10                      | 1.06                       | -    |
| 4     | 4     | 45.50                        | 16.69                      | 1.87                       | +    |
| 5     | 1     | 46.17                        | 14.54                      | 1.45                       | -    |
| 5     | 3     | 315.02                       | 12.95                      | 1.52                       | +    |
| 6     | 4     | 193.19                       | 9.52                       | 1.32                       | +    |
| 7     | 3     | 56.13                        | 11.20                      | 1.62                       | +    |
| 7     | 4     | 82.43                        | 4.28                       | 0.65                       | -    |
| 7     | 5     | 48.68                        | 7.89                       | 1.27                       | -    |
| 8     | 6     | 34.97                        | 8.13                       | 1.53                       | -    |
| 9     | 5     | 92.69                        | 8.80                       | 1.70                       | -    |
| 9     | 6     | 51.38                        | 3.34                       | 0.68                       | +    |
| 10    | 6     | 41.41                        | 1.80                       | 0.39                       | +    |
| 11    | 7     | 158.35                       | 7.02                       | 1.75                       | +    |
| 12    | 7     | 43.05                        | 2.66                       | 0.71                       | -    |
| 13    | 8     | 74.22                        | 3.00                       | 0.89                       | +    |
| 16    | 10    | 80.05                        | 3.32                       | 1.30                       | +    |
| 18    | 11    | 76.01                        | 3.18                       | 1.46                       | -    |

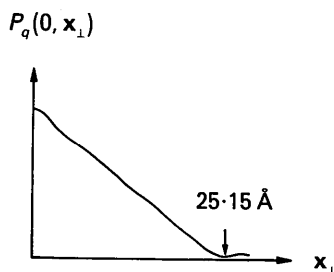


Fig. 2. Origin peak of  $P_q(0, \mathbf{x}_\perp)$ .

In order to evaluate  $S(\mathbf{H}_\perp)$ , we need the value of  $l_1 + l_2$ . As discussed in the previous section, the Patterson-origin peak will fall to a minimum as  $|\mathbf{x}_\perp|$  increases from 0 to  $l_1 + l_2$ , the width of  $w(\mathbf{x}_\perp)$ . A Patterson section  $P_q(0, \mathbf{x}_\perp)$  was calculated using  $|\mathbf{F}_q(\hat{\mathbf{H}})|^2$  as coefficients. The origin peak falls to the base line at about  $25.15 \text{ \AA}$ , as shown in Fig. 2. Hence, as a first approximation we have  $l_1 + l_2 = 25.15 \text{ \AA}$ . This value can be refined by the following trial-and-error procedure. With a value of  $l_1 + l_2$ , we can convert  $|\mathbf{F}_q(\hat{\mathbf{H}})|$  to the corresponding  $|\mathbf{F}(\hat{\mathbf{H}})|$  and then calculate the normalized structure-factor amplitudes  $|\mathbf{E}(\hat{\mathbf{H}})| = |\mathbf{F}(\hat{\mathbf{H}})| / (\sum f_j^2)^{1/2}$ , where  $f_j$  is the atomic scattering factor for electrons in the 3D physical space. A Patterson function  $P_E(\mathbf{x}, \mathbf{x}_\perp)$  calculated with  $|\mathbf{E}(\hat{\mathbf{H}})|^2$  as coefficients will correspond to a self-convolution of a point-atom structure and should have in theory a delta-function-like origin peak. If the value of  $l_1 + l_2$  is not accurate enough, then the origin peak of  $P_E(\mathbf{x}, \mathbf{x}_\perp)$  will be broadened. By changing the value of  $l_1 + l_2$  in small steps we can find the best value which makes the origin peak of  $P_E(\mathbf{x}, \mathbf{x}_\perp)$  the sharpest one. In this way, starting from  $l_1 + l_2 = 25.15 \text{ \AA}$  we obtained a refined value  $l_1 + l_2 = 24.76 \text{ \AA}$  which is much closer to the true value  $24.77 \text{ \AA}$ . Patterson maps corresponding to these three values of  $l_1 + l_2$  are shown in Fig. 3. As can be seen even in the  $P_E(\mathbf{x}, \mathbf{x}_\perp)$  calculated with the true value of  $l_1 + l_2$ , peaks are elongated along  $\mathbf{x}_\perp$ . This is due to the truncation effect in pseudo-space. Further discussion will be given later. A set of  $|\mathbf{F}(\hat{\mathbf{H}})|$  and the corresponding  $|\mathbf{E}(\hat{\mathbf{H}})|$  values calculated with  $l_1 + l_2 = 24.76 \text{ \AA}$  are listed in Table 2.

### B. Phase (sign) derivation

A multi-solution direct-method procedure was applied to the  $|\mathbf{E}(\hat{\mathbf{H}})|$ 's listed in Table 2. Random starting signs were assigned to seven reflections at the

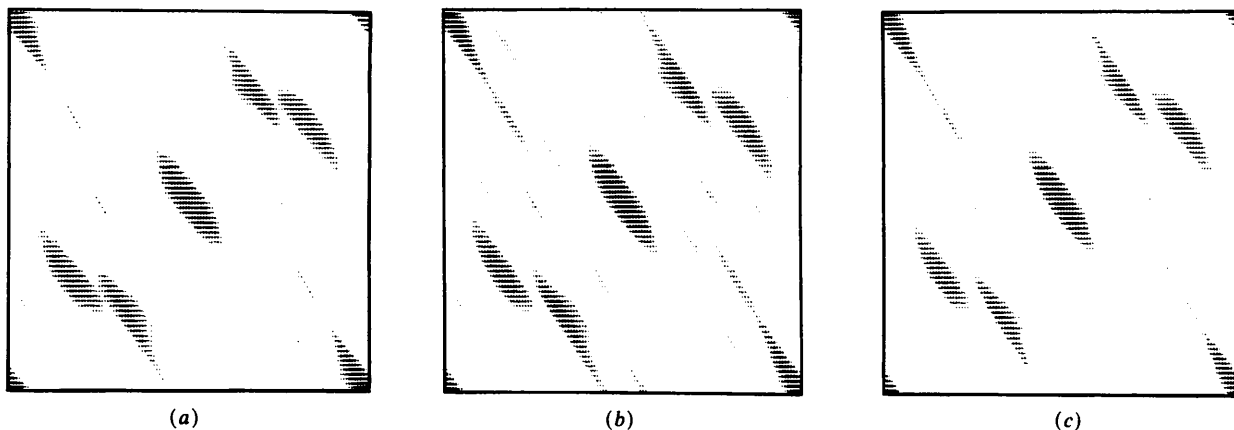


Fig. 3. Patterson maps  $P_E(\mathbf{x}, \mathbf{x}_\perp)$  calculated according to different values of  $l_1 + l_2$ . (a)  $l_1 + l_2 = 25.15$ ; (b)  $l_1 + l_2 = 24.77$  (the true value); (c)  $l_1 + l_2 = 24.76 \text{ \AA}$ .  $\mathbf{x}_1$  is horizontal,  $\mathbf{x}_2$  up the page, and  $\mathbf{x}_\perp$  along the long axes of the elliptical regions.

bottom of the convergence map. 50 trials were calculated. The best result was picked by using the residual figure of merit defined as

$$R_\alpha = \sum_{\hat{H}} |\alpha_{est} - \alpha| / \sum_{\hat{H}} \alpha_{est},$$

where

$$\alpha^2 = \left( \sum_{\hat{H}'} \kappa \cos \Phi \right)^2 + \left( \sum_{\hat{H}'} \kappa \sin \Phi \right)^2,$$

$$\alpha_{est} \sim \sum_{\hat{H}'} \kappa [I_1(\kappa) / I_0(\kappa)],$$

$$\kappa = 2\sigma_3 \sigma_2^{-3/2} |E(\hat{H})E(\hat{H}')E(\hat{H} - \hat{H}')|,$$

$$\Phi = \varphi_{\hat{H}'} + \varphi_{\hat{H} - \hat{H}'}.$$

For the theory of convergence map and figures of merit, the reader is referred to papers by Germain, Main & Woolfson (1970, 1971).  $R_\alpha$  values resulting from the 50 random trials range from 0.170 to 0.519. There were nine trials having  $R_\alpha$  equal to the minimum value 0.170. All these nine trials led to the correct solution of the structure with signs of the total 26 reflections correctly determined. The corresponding  $E$  map is shown in Fig. 4. Atomic positions of

the 1D quasicrystal were measured from the peak positions of the  $E$  map and are listed in Table 1.

### Discussion

A common feature in quasicrystal and incommensurate modulated structures is that atoms spread out in pseudo-space along each pseudo-axis. In the case of incommensurate modulated structures, the pseudo-axes are also axes of the corresponding MD crystal. Atoms having a shape in pseudo-space determined by the modulation function will not overlap one another, while in the case of quasicrystal structures, the pseudo-axes are not parallel to those of the corresponding MD crystal. Atoms have a shape in pseudo-space determined by the shape factor  $S(\mathbf{H}_\perp)$ . These extended atoms may overlap one another. Hence before applying direct methods to solve the phase problem it is essential to correct the shape factor, *i.e.* to convert  $|\mathbf{F}_q(\hat{H})|$  to  $|\mathbf{F}(\hat{H})|$ . This is equivalent to sharpening the atoms to geometrical points in pseudo-space. In view of this the evaluation of  $S(\mathbf{H}_\perp)$  is an important step for applying direct methods to quasicrystals. As can be seen from Figs. 2 and 3 the method proposed in this paper for evaluating  $S(\mathbf{H}_\perp)$  is easy to implement and very efficient.

It should be noticed that in practice we cannot obtain a complete set of  $|\mathbf{F}(\hat{H})|$  from a set of experimental data  $|\mathbf{F}_q(\hat{H})|$ , since as  $|\mathbf{H}_\perp|$  increases,  $S(\mathbf{H}_\perp)$  decreases rapidly; thus according to (3) the value of  $|\mathbf{F}_q(\hat{H})|$  will also decrease rapidly. For this reason it is not possible in practice to observe  $|\mathbf{F}_q(\hat{H})|$  with large  $|\mathbf{H}_\perp|$ . Consequently  $|\mathbf{F}_q(\hat{H})|$  and also  $|\mathbf{F}(\hat{H})|$  will suffer from serious truncation in pseudo-reciprocal space. This explains that even after correcting the shape factor, peaks in Figs. 3 and 4 are still elongated, of course to a much smaller extent, along  $\mathbf{x}_\perp$ .

The resemblance of Figs. 4(a) and (b) shows that the direct phasing of quasicrystal diffraction data was successful in spite of the serious truncation of diffraction data. However the direct-method technique used in the test is just a routine procedure in X-ray crystallography. It can be further improved to suit quasicrystal structure analysis.

For the example used in this paper Patterson analysis can also be used to derive the quasicrystal structure. As can be seen from Fig. 3, after correcting the shape factor it is not difficult to solve the 2D structure by Patterson analysis. However, when the quasicrystal becomes more complicated, especially when it is composed of nearly equal atoms, direct methods will then be superior to Patterson analysis. Hence we recommend the combination of Patterson and direct methods. The former is used to evaluate  $S(\mathbf{H}_\perp)$ , while the latter is used to derive the phases.

Although the test was done on a 1D quasicrystal model with simple arrangement of atoms, there is no theoretical limitation to the procedures for use in the

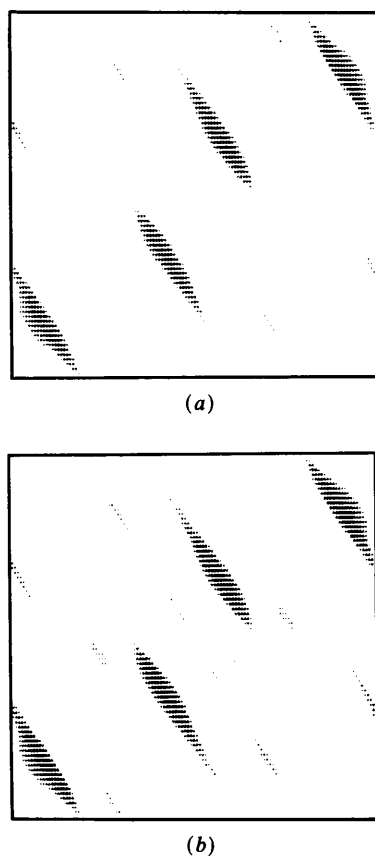


Fig. 4.  $E$  maps of the 2D crystal. (a)  $E$  map resulting from the direct method. (b) Theoretical  $E$  map of the model structure. Axes as in Fig. 3.

multi-dimensional case with more complicated atomic arrangements.

#### References

BAK, P. (1986). *Phys. Rev. Lett.* **56**, 861–864.

GERMAIN, G., MAIN, P. & WOOLFSON, M. M. (1970). *Acta Cryst.* **B26**, 274–285.

GERMAIN, G., MAIN, P. & WOOLFSON, M. M. (1971). *Acta Cryst.* **A27**, 368–376.

HAO QUAN, LIU YI-WEI & FAN HAI-FU (1987). *Acta Cryst.* **A43**, 820–824.

JANSSEN, T. (1986). *Acta Cryst.* **A42**, 261–271.

LI FANG-HUA, WANG LI-CHEN & FAN HAI-FU (1987). *Mater. Sci. Forum*, **22–24**, 397–408.

SHECHTMAN, D., BLECH, I., GRATIAS, D. & CAHN, J. W. (1984). *Phys. Rev. Lett.* **53**, 1951–1953.

WOOLFSON, M. M. (1987). *Acta Cryst.* **A43**, 593–612.

*Acta Cryst.* (1990). **A46**, 478–485

## A Synchrotron X-ray Study of the Surface Layer in Stoichiometric LiNbO<sub>3</sub> on Modulation by an Applied Electric Field\*

BY KENNY STÅHL

*Inorganic Chemistry 2, University of Lund, PO Box 124, S-221 00 Lund, Sweden*

ÅKE KVICK†

*Chemistry Department, Brookhaven National Laboratory, Upton, New York 11973, USA*

AND S. C. ABRAHAMS

*AT&T Bell Laboratories, Murray Hill, New Jersey 07974, USA and Institut für Kristallographie der Universität Tübingen, Charlottenstrasse 33, D-7400 Tübingen, Federal Republic of Germany*

(Received 24 April 1989; accepted 16 January 1990)

### Abstract

A single crystal of stoichiometric lithium niobate has been studied, using high-resolution synchrotron X-rays, under an electric field applied along the polar crystallographic *c* direction. A crystalline plate, 0.2 mm thick along the *c* direction, was polarized by a  $\pm 900$  V square wave of frequency 50 and 230 Hz. Electronic gating ensured that the scattered intensities were recorded only during the central 50% of the square-wave duration. The results show that the stoichiometric crystals have surface layers under the Al electrodes that differ in the *c* cell dimension from the bulk by about  $\Delta c/c = 6 \times 10^{-4}$ . The resulting *c* lattice vector is close in length to that of congruent Li<sub>0.941</sub>Nb<sub>1.012</sub>O<sub>3</sub>, although the composition of the surface layer may only be inferred; modification by Al in-diffusion may also be possible. The surface-layer thickness is estimated to be of the order of 0.01 mm.

### Introduction

Lithium niobate is a readily grown high-quality single-crystal material widely used in many electronic and electro-optic devices. A detailed review of the chemistry and physics of lithium niobate has been given by Räuber (1978) and, more recently, in *Properties of Lithium Niobate* (EMIS, 1989). A detailed study of both the congruent and stoichiometric crystal structure has been presented by Abrahams & Marsh (1986).

Lithium niobate has a congruent melting point at 1513 K corresponding to the chemical composition Li<sub>0.946</sub>NbO<sub>2.973</sub> (Carruthers, Peterson, Grasso & Bridenbaugh, 1971), as found in single crystals grown from the melt. It is however possible to form stoichiometric crystals by lithium vapor-phase equilibration of congruent material for about 800 h at 1373 K (O'Bryan, Holmes & Kim, 1984). The physical properties of lithium niobate are strongly dependent on composition; for instance, the congruent phase has a ferroelectric Curie temperature  $T_c = 1402$  K, whereas the stoichiometric phase has the considerably higher  $T_c$  of 1471 (2) K (Gallagher & O'Bryan, 1985).

\* This research was carried out at Brookhaven National Laboratory under contract DE-AC02-76CH00016 with the US Department of Energy and supported by its Division of Chemical Sciences, Office of Basic Energy Sciences.

† Present address: European Synchrotron Radiation Facility, BP 220, F-38043 Grenoble CEDEX, France.